PERGAMON

International Journal of Solids and Structures 38 (2001) 6163–6182

INTERNATIONAL JOURNAL OF SOLIDS and STRUCTURES

www.elsevier.com/locate/ijsolstr

Analysis of laminated circular cylinders of materials with the most general form of cylindrical anisotropy. I. Axially symmetric deformations

C.H. Huang [a], S.B. Dong [b,*]

[a] *Department of Civil Engineering, National Taipei University of Technology, Taipei, Taiwan*

[b] *Department of Civil and Environmental Engineering, University of California, Los Angeles, CA 90095-1593, USA*

Received 22 September 1999; in revised form 28 September 2000

Abstract

A procedure is presented for the analysis of stresses and deformations in a laminated circular cylinder of perfectly bonded materials with the most general form of cylindrical anisotropy. Attention is focused in this paper on axisymmetric loads, and a companion paper will be devoted to loads producing flexural deformations. Axisymmetric loading conditions include an axial force and torque on the ends as well as a general distribution of surface tractions of pressure, circumferential shear and longitudinal shear. These surface tractions are represented by a power series in the axial coordinate. Only the leading two terms are considered herein; they relate to uniform and linear variations of the normal pressures and uniform circumferential and longitudinal surface shears. From the methodology for these two terms, extension of the analysis procedure for higher terms will be readily apparent. The solutions herein fit descriptions of (1) the relaxed formulation of Saint-Venant's problem where prescribed tractions on the ends on a point-wise basis are replaced by integral conditions relating to an axial force and torque and (2) the Almansi–Michell problem. Differences in the stress distributions between these integral conditions with any point-wise specification are self-equilibrated states that evanesce with distance from the ends, i.e., Saint-Venant's principle, and some remarks are offered for treatment of such effects.

Keywords: Circular cylinder; Anisotropy; Axisymmetric elastostatics

1. Introduction

In the stress analysis of a circular cylinder fabricated from fiber composite materials, the applicable structural theory depends on its radius/thickness ratio R/H. For a *thin-walled* cylinder, i.e., $R/H \gg 1$, either classical or first order shear deformation shell theory is capable of accurately predicting its behavior. See Noor et al. (1991) for a survey of such studies. For R/H small (say $R/H < 10$), three-dimensional (3D) elasticity must be used. The literature on 3D elasticity analyses of cylinders is abundant, but most of it is

* Corresponding author. Address: School of Engineering and Applied Science, University of California, 405 Hilgara Avenue, Los Angles, California 90024-1600, USA. Tel.: +1-310-825-5353; fax: +1-310-206-2222.

E-mail address: dong@seas.ucla.edu (S.B. Dong).

0020-7683/01/$ - see front matter
PII: S0020-7683(00)00374-7

devoted to isotropic and orthotropic cylinders: for examples, see Shaffer (1968), Chou and Achenbach (1972), Noor and Rarig (1974), Srinivas (1974), Grigorenko et al. (1974), Chandrashekhara and Gopalakrishnan (1982), Hyer et al. (1986), Ren (1987), Hyer (1988), Roy and Tsai (1988), Noor and Peters (1989), Spencer et al. (1990), Varadan and Bhaskar (1991), and Ye and Soldatos (1994). For monotropic and anisotropic cylinders, 3D elasticity analysis is disproportionately more cumbersome than for the aforementioned cases. Examples of monotropic cylinder analyses include Sherrer (1967), Pagano (1972), Hyer and Rousseau (1987), Lee and Springer (1990), Kollar (1994), Kollar and Springer (1992), Kollar and Patterson (1993) and Kollar et al. (1992). Some fundamental results for a homogeneous circular cylinder with the most general form of cylindrical anisotropy are also available; expressions for a stress state which does not vary along the generating axis are summarized in Lekhnitskii (1981) text. Lekhnitskii used the Airy and Prandtl stress functions, an approach that does not provide displacements without further integrations. Displacement data were given by Sherrer (1967), Pagano (1972), Hyer and Rousseau (1987), Kollar (1994), Kollar and Springer (1992), Kollar and Patterson (1993) and Kollar (1994) in their monotropic cylinder analyses.

This synopsis of the state-of-the-art reveals that a tractable method for the analysis of a multilayered cylinder of materials with cylindrical anisotropy of the most general form (i.e., 21 distinct elastic constants per material) remains to be developed. While construction of an analytical solution for this case is deceivingly straight-forward (i.e., by linking single-layer anisotropic cylinder results according to full interlaminar traction and displacement continuity and prescribed lateral surface conditions), the algebra is formidable. Kollar et al.'s consideration of the case of a multilayered monotropic cylinder under the condition of the stresses remaining constant along the generating axis (Kollar, 1994; Kollar and Springer, 1992; Kollar and Patterson, 1993) exemplifies the extent of the details involved.

An analysis based on 3D elasticity of a general laminated circular cylinder under arbitrary axisymmetric loading conditions is presented herein. The cylinder's radial profile may consist of any number of perfectly bonded layers, each having its own thickness and distinct cylindrically anisotropic mechanical properties, where the anisotropy may be of the most general form, i.e., 21 independent elastic moduli or compliances. The analysis is based on semi-analytical finite elements, and in the present version, the governing equations are ordinary differential equations in terms of the axial coordinate. Two axisymmetric loading conditions are considered, which induce uniform and linear variations of stress along the axis of the cylinder. Solutions for loadings inducing higher variations of stress states can be inferred by induction from the method for these two cases. The solution procedure calls for setting forth the general form of the displacement fields at the outset, and analysis enables these fields to be completely defined. The problem statement and solution for the uniform stress state fit the relaxed formulation of the Saint-Venant (1856a,b) problem, and that for the linearly varying stress state is associated with the Almansi (1901a,b) Michell (1901) problem. Remarks on the modification of these solution to account for point-wise specification of end conditions are offered in the concluding remarks. Such end effects fall within the realm of the quantitative analysis of Saint-Venant's principle. In a companion paper, the present methodology will be applied to flexural loading conditions.

2. Basic equations

Consider a circular cylinder of length L with a radial profile consisting of any number of perfectly bonded elastic layers, each with distinct cylindrical anisotropic mechanical properties and thickness. Let this cylinder be restrained from translation and rotation at one end (the fixed end) and unsupported at the other (the tip end). Adopt cylindrical coordinates (r, θ, z) and with the origin at the center of the tip end cross-section as shown in Fig. 1a. Let r_0 denote the outer radius, and if the cylinder is hollow, let r_i denote the radius of its inner lateral surface. The components of displacement vector, stress and strain are, respectively, $\bar{\mathbf{u}} = [u, v, w]$, $\boldsymbol{\sigma} = [\sigma_{rr}, \sigma_{\theta\theta}, \sigma_{zz}, \sigma_{\theta z}, \sigma_{rz}, \sigma_{r\theta}]^{\mathrm{T}}$, and $\boldsymbol{\epsilon} = [\epsilon_{rr}, \epsilon_{\theta\theta}, \epsilon_{zz}, \gamma_{\theta z}, \gamma_{rz}, \gamma_{r\theta}]^{\mathrm{T}}$. The constitutive relation for any layer in the laminated cylinder is

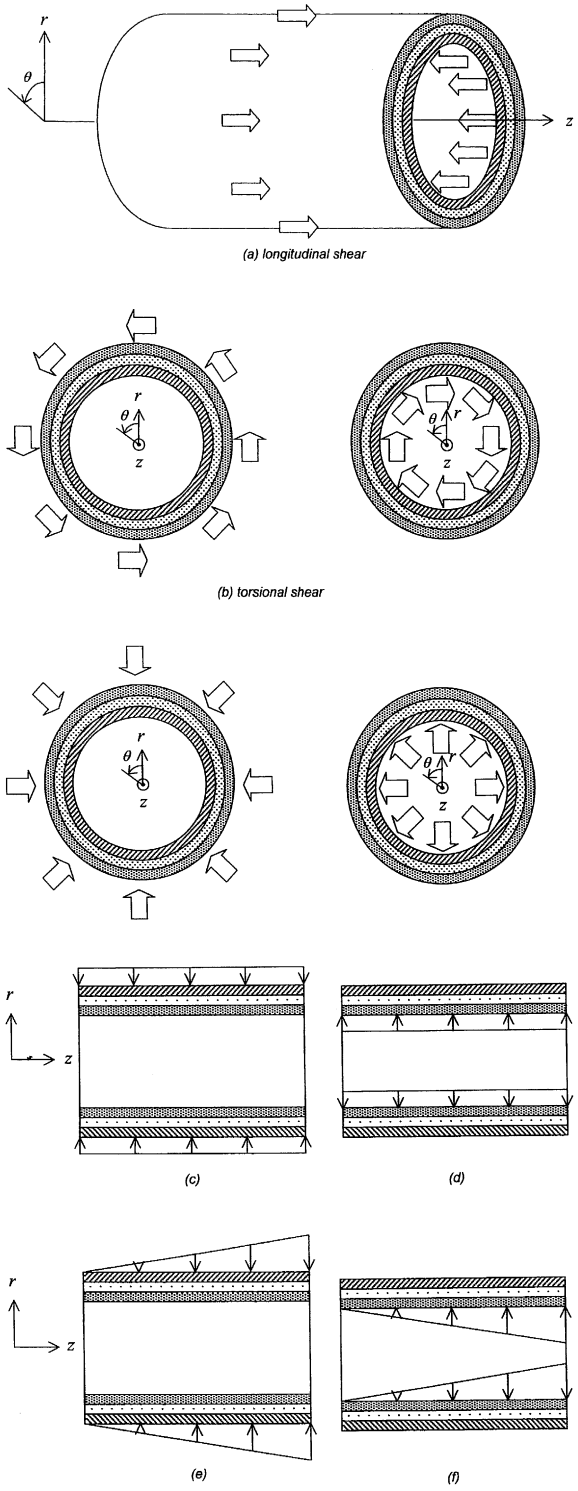

Fig. 1. (a) Circular cylinder under uniform axial and torsion shears. (b) Circular cylinder under uniform and linear pressurizations.

$$\boldsymbol{\sigma} = \mathbf{C}\boldsymbol{\epsilon}, \tag{1}$$

where $\mathbf{C}$ is a (6×6) matrix of cylindrically anisotropic elastic moduli with the anisotropy axis coinciding with the z-axis (or 3-axis). For a solid cylinder, the properties as $r \to 0$ must exhibit a transition from anisotropy to transverse isotropy in order for a physically meaningful axisymmetric structure, i.e., $C_{11} = C_{22}$, $C_{13} = C_{23}$, $C_{44} = C_{55}$. No such restrictions are necessary if the cylinder is hollow.

The semi-analytical finite element equations to be used herein appeared previously in Zhuang et al. (1999). Hence, only its essence need to be summarized here, and many of their details may be omitted. In this semi-analytical finite element version, the thickness profile of the cylinder undergoes discretization radially into cylindrical laminas. Each lamina is a separate entity enjoying distinct mechanical properties and thickness, so that a collection of such elements is suitable for representing any laminated, anisotropic cylinder. Within each lamina, the radial dependence of the displacement field $\overline{\mathbf{u}}$ is represented by quadratic interpolations over three equally spaced nodal surfaces, i.e.,

$$\begin{bmatrix} u(r,\theta,z) \\ v(r,\theta,z) \\ w(r,\theta,z) \end{bmatrix} = \begin{bmatrix} \mathbf{n}(r) & \cdot & \cdot \\ \cdot & \mathbf{n}(r) & \cdot \\ \cdot & \cdot & \mathbf{n}(r) \end{bmatrix} \begin{bmatrix} u(\theta,z) \\ v(\theta,z) \\ w(\theta,z) \end{bmatrix} \quad \text{or} \quad \overline{\mathbf{u}}(r,\theta,z) = \overline{\mathbf{n}}(r)\mathbf{u}(\theta,z), \tag{2}$$

where $\{u, v, w\}$ are (3×1) arrays of the nodal displacement components whose axial and circumferential dependencies are unspecified at the outset and $\mathbf{n}$'s are the radial interpolations.

This form of the displacement field for a generic lamina requires that linear strain-displacement equations be split into differentiations with respect to r,θ,z.

$$\boldsymbol{\epsilon} = (\mathbf{L}_r + \mathbf{L}_\theta + \mathbf{L}_z)\overline{\mathbf{u}}, \tag{3}$$

where $(\mathbf{L}_r, \mathbf{L}_\theta, \mathbf{L}_z)$ are 6×3 differential operator matrices. Inserting displacement field (2) into Eq. (3) leads to the following strain-transformation equations.

$$\boldsymbol{\epsilon} = \mathbf{b}_r\mathbf{u} + \mathbf{b}_\theta\mathbf{u}_{,\theta} + \mathbf{b}_z\mathbf{u}_{,z}\,. \tag{4}$$

Both strain-displacement operators $\mathbf{L}_i$'s and strain-transformation matrices $\mathbf{b}_i$'s are given in Zhuang et al. (1999).

Varying the total strain energy, from computing the elemental strains by Eq. (4) and summing them, leads to the following set of discrete partial differential equations

$$\mathbf{K_1}\mathbf{U} + \mathbf{K_2}\mathbf{U}_{,\theta} + \mathbf{K_3}\mathbf{U}_{,z} - \mathbf{K_4}\mathbf{U}_{,\theta\theta} - \mathbf{K_5}\mathbf{U}_{,\theta z} - \mathbf{K_6}\mathbf{U}_{,zz} = \mathbf{F}(\theta,z), \tag{5}$$

where $\mathbf{U}(\theta,z)$ is the assembled $(3N \times 1)$ array of all nodal displacement components at the N nodes of the finite element model, $\mathbf{K_i}$'s are system stiffness matrices, [1] and $\mathbf{F}(\theta,z)$ is the consistent load vector. The set of equilibrium equations (5) is valid for both axisymmetric and nonsymmetric loading conditions.

3. Equations for axisymmetric deformations

Axisymmetric deformations are independent of θ and Eq. (5) reduces to

$$\mathbf{K_1}\mathbf{U}(z) + \mathbf{K_3}\mathbf{U}_{,z}(z) - \mathbf{K_6}\mathbf{U}_{,zz}(z) = \mathbf{F}(z), \tag{6}$$

where $\mathbf{F}(z)$ represents pressure loads on the cylinder's inner and outer lateral surfaces.

[1] These matrices may be found in Zhuang et al. (1999). It is noted that $\mathbf{K_1}$, $\mathbf{K_4}$, $\mathbf{K_5}$ and $\mathbf{K_6}$ are symmetric, while $\mathbf{K_2}$ and $\mathbf{K_3}$ are antisymmetric.

The strategy for solving Eq. (6) relies on representing $\mathbf{F}$ as a power series in z.

$$\mathbf{F}(z) = \mathbf{F}_0 + z\mathbf{F}_1 + \cdots + z^k\mathbf{F}_k, \tag{7}$$

where $\mathbf{F}_0$ embodies uniform internal and external pressures, $z\mathbf{F}_1$ defines the linear varying pressures, and subsequent terms represent higher order polynomial pressure gradients. Consequently, the displacement field can be taken as

$$\mathbf{U}(z) = \mathbf{U}_0(z) + \mathbf{U}_1(z) + \cdots + \mathbf{U}_k(z), \tag{8}$$

where each term $\mathbf{U}_j(z)$ is associated with the corresponding load term $z^j\mathbf{F}_j$ in Eq. (7). Displacement field $\mathbf{U}_0(z)$ embodies strain and stress fields that are uniform in the axial direction. This state represents a cylinder under uniform internal and external pressure with the possibility of equal and opposite axial forces and torques acting on the two ends. The next term $\mathbf{U}_1(z)$ gives strain and stress fields that are at most linear in z and appropriate for (1) linearly varying normal pressures and (2) uniform axial and circumferential surface shear tractions. Successively higher displacement terms define higher axial variations of the strain and stress fields for correspondingly higher polynomial variations of the loading conditions.

As the relaxed formulation of the problem is considered herein, end conditions in terms of axial force P_z and torque M_z are used. These resultants are given by integrals of end tractions σ_{zz} and $\sigma_{\theta z}$ over the cross-section.

$$P_z = 2\pi \int_{r_i}^{r_0} \sigma_{zz}\, r\, \mathrm{d}r; \qquad M_z = 2\pi \int_{r_i}^{r_0} \sigma_{\theta z}\, r^2\, \mathrm{d}r. \tag{9}$$

A solution using a *point-wise* prescription of the end conditions differs with that based on integral conditions (9) only in the region near the ends according to Saint-Venant's principle. Means to modify the solutions herein to account for such end effects are addressed in the concluding remarks.

Only the first two terms, i.e., $\mathbf{U}_0(z)$ and $\mathbf{U}_1(z)$, for uniform and linearly varying strain and stress fields are considered herein and they are denoted as Problems I and II. From their discussion, the treatment of higher terms will become apparent.

4. Rigid body displacements

The rigid body motions of translation w_0 and rotation ω_3 about the z-axis when substituted into the homogeneous form of Eq. (6) must satisfy it identically. Also, its substitution into strain-transformation Eq. (6) yields zero strain. These relations provide identities that are used in the solution procedure and are set forth here. Let $\mathbf{U_{RB}}$ be the vector of rigid body translation w_0 and rotation ω_3 about the z-axis.

$$\mathbf{U_{RB}} = w_0\mathbf{R_3} + \omega_3\mathbf{R_4}, \tag{10}$$

where

$$\mathbf{U_{RB}} = [\boldsymbol{U}, \boldsymbol{V}, \boldsymbol{W}]^{\mathrm{T}}; \qquad \mathbf{R_3} = [\mathbf{0}, \mathbf{0}, \mathbf{I}]^{\mathrm{T}}; \qquad \mathbf{R_4} = [\mathbf{0}, \mathbf{R}, \mathbf{0}]^{\mathrm{T}} \tag{11}$$

with column vectors $\mathbf{I}$ and $\mathbf{R}$ containing unit entries and the r-coordinate of the nodes, respectively. Substituting Eq. (10) into Eqs. (6) and (4) and equating the bracketed quantities of w_0 and ω_3 to zero give

$$\mathbf{K_1R_3} = \mathbf{0}; \qquad \mathbf{K_1R_4} = \mathbf{0} \quad \text{and} \quad \mathbf{b}_r\mathbf{r_3} = \mathbf{0}; \qquad \mathbf{b}_r\mathbf{r_4} = \mathbf{0}, \tag{12}$$

where $\mathbf{r_3}$ and $\mathbf{r_4}$ are element level vectors that correspond to $\mathbf{R_3}$ and $\mathbf{R_4}$.

5. Problem I – uniform stress state

The displacement and load vectors, $\mathbf{U}_0(z)$ and $\mathbf{F}_0$, satisfy the equation

$$\mathbf{K_1}\mathbf{U}_0 + \mathbf{K_3}\mathbf{U}_{0,z} - \mathbf{K_6}\mathbf{U}_{0,zz} = \mathbf{F}_0, \tag{13}$$

where $\mathbf{F}_0$ contains the internal and external pressures p_{ri} and p_{r0} as shown in Fig. 1b. In addition to these pressurizations, there may be equal and opposite axial forces P_z and torques M_z on the two end cross-sections. For this loading condition, the strain and stress states are uniform in the z-direction, and the most general form of the displacement field is given by

$$\begin{aligned} u_0 &= a_{I3}\Psi_{Iu3}(r) + a_{I6}\Psi_{Iu6}(r) + u_{I\mathrm{p}}(r), \\ v_0 &= a_{I6}rz + a_{I3}\Psi_{Iv3}(r) + a_{I6}\Psi_{Iv6}(r) + v_{I\mathrm{p}}(r) + \omega_3 r, \\ w_0 &= a_{I3}z + a_{I3}\Psi_{Iw3}(r) + a_{I6}\Psi_{Iw6}(r) + w_{I\mathrm{p}}(r) + w_0, \end{aligned} \tag{14a}$$

or in matrix notation in terms of the nodal variables of the finite element model as

$$\mathbf{U}_0 = a_{I3}[z\boldsymbol{R}_3 + \boldsymbol{\Psi}_{I3}] + a_{I6}[z\boldsymbol{R}_4 + \boldsymbol{\Psi}_{I6}] + \mathbf{U}_{I\mathrm{p}} + \omega_3\mathbf{R}_4 + w_0\mathbf{R}_3, \tag{14b}$$

where

$$\mathbf{U}_0 = \begin{Bmatrix} \boldsymbol{U}_0 \\ \boldsymbol{V}_0 \\ \boldsymbol{W}_0 \end{Bmatrix}, \qquad U_{I\mathrm{p}} = \begin{Bmatrix} \boldsymbol{U}_{I\mathrm{p}} \\ \boldsymbol{V}_{I\mathrm{p}} \\ \boldsymbol{W}_{I\mathrm{p}} \end{Bmatrix}, \qquad \boldsymbol{\Psi}_{Ii} = \begin{Bmatrix} \boldsymbol{\psi}_{Iui} \\ \boldsymbol{\psi}_{Ivi} \\ \boldsymbol{\psi}_{Iwi} \end{Bmatrix} \tag{15}$$

and $\mathbf{R}_3$ and $\mathbf{R}_4$ were given in Eq. (11). The coefficients [2] a_{I3} and a_{I6} are amplitudes whose values depend on axial force P_z and torque M_z. The polynomial terms z and rz of the w and v displacement components are termed the *primal field*. They represent plane longitudinal deformation and pure twisting of the circular cylinder, the familiar kinematic hypotheses of elementary theory. The terms $\boldsymbol{\Psi}_{I3}$ and $\boldsymbol{\Psi}_{I6}$ are the cross-sectional deformations due to Poisson's ratio effects and extension-torsional coupling when the cylinder is composed of laminated anisotropic materials. All of these deformations are collectively called the *warpages*. The term $\mathbf{U}_{I\mathrm{p}}$ is the particular solution of Eq. (13) for the applied pressures. Displacement field (14a) and (14b) can be established by integrating the strain-displacement equations for a longitudinally uniform strain state. It can also be obtained by integrating rigid body displacement (10) once with respect to z and adopting the kinematic coefficients a_{I3} and a_{I6} for the integrated field. This latter method of generating $\mathbf{U}_0$ is due to Iesan (1986, 1987). The remaining terms involving w_0 and ω_3 are the rigid body motions.

Substituting displacement field (14b) into governing Eq. (13) yields

$$za_{I3}\{\mathbf{K_1}\mathbf{R_3}\} + za_{I6}\{\mathbf{K_1}\mathbf{R_4}\} + \{\mathbf{K_1}\mathbf{U}_{I\mathrm{p}} - \mathbf{F}_0\} + a_{I3}\{\mathbf{K_1}\boldsymbol{\Psi}_{I3} + \mathbf{K_3}\mathbf{R_3}\} + a_{I6}\{\mathbf{K_1}\boldsymbol{\Psi}_{I6} + \mathbf{K_3}\mathbf{R_4}\} = 0. \tag{16}$$

For Eq. (16) to be satisfied, each term enclosed by braces must vanish by itself. The two terms involving z are satisfied because of rigid body displacement identities (12). Setting the remaining terms equal to zero gives

$$\mathbf{K_1}\boldsymbol{\Psi}_{I3} = -\mathbf{K}_3 R_3, \qquad \mathbf{K_1}\boldsymbol{\Psi}_{I6} = -\mathbf{K}_3 R_4, \qquad \mathbf{K_1}\mathbf{U_{Ip}} = \mathbf{F}_0. \tag{17}$$

The solutions to Eq. (17) define the displacement field completely except for amplitudes a_{I3} and a_{I6}. It is noted that $\mathbf{K_1}$ is singular, and two degrees of freedom, an axial translation and a rotation about the z-axis, must be restrained before its inversion is possible. This suppression may take the form of deleting an axial and a circumferential degree of freedom or by condensing these two rigid body motions from $\mathbf{K_1}$. Removing

[2] Subscripts 3 and 6 are used for the force and moment in the z-direction. Subscripts 1, 2, 4, 5 are reserved for forces and moments about two orthogonal axes in the plane of the cross-section.

any two of these degrees of freedom does not alter the relative displacements due to deformation, as a rigid body displacement can always be appended to the deformed geometry to meet the boundary conditions on the fixed end of the cylinder. For the case of a solid cylinder, the displacements on the z-axis must vanish, i.e., $u(0,z) = v(0,z) = 0$.

Knowing all the components of $\mathbf{U}_0$, the strains and stresses are found by means of Eqs. (4) and (1).

$$\boldsymbol{\epsilon} = a_{I3}\boldsymbol{\epsilon}_{I3} + a_{I6}\boldsymbol{\epsilon}_{I6} + \boldsymbol{\epsilon}_{I\mathrm{p}}, \qquad \boldsymbol{\sigma} = a_{I3}\boldsymbol{\sigma}_{I3} + a_{I6}\boldsymbol{\sigma}_{I6} + \boldsymbol{\sigma}_{I\mathrm{p}}, \tag{18}$$

where

$$\begin{aligned} &\boldsymbol{\epsilon}_{I3} = \mathbf{b}_r\boldsymbol{\Psi}_{I3} + \mathbf{b}_z\mathbf{r}_3, \qquad \boldsymbol{\epsilon}_{I6} = \mathbf{b}_r\boldsymbol{\psi}_{I6} + \mathbf{b}_z\mathbf{r}_4, \qquad \boldsymbol{\epsilon}_{I\mathrm{p}} = \mathbf{b}_r\mathbf{u}_{I\mathrm{p}} \\ &\boldsymbol{\sigma}_{I3} = \mathbf{C}\boldsymbol{\epsilon}_{I3}, \qquad \boldsymbol{\sigma}_{I6} = \mathbf{C}\boldsymbol{\epsilon}_{I6}, \qquad \boldsymbol{\sigma}_{I\mathrm{p}} = \mathbf{C}\boldsymbol{\epsilon}_{I\mathrm{p}} \end{aligned} \tag{19}$$

Coefficients a_{I3} and a_{I6} are determined by equating the integrals of the stresses over the cross-section for P_z and M_z to the applied axial force and torque, P_0 and M_0. Substituting σ_{zz} and $\sigma_{\theta z}$ from third and fourth lines of Eq. (18) into Eq. (9) gives

$$\begin{bmatrix} \kappa_{I33} & \kappa_{I36} \\ \kappa_{I63} & \kappa_{I66} \end{bmatrix} \begin{Bmatrix} a_{I3} \\ a_{I6} \end{Bmatrix} + \begin{Bmatrix} P_{I1} \\ M_{I1} \end{Bmatrix} = \begin{Bmatrix} P_0 \\ M_0 \end{Bmatrix}, \tag{20}$$

where κ_{Iij} $(i,j = 3,6)$ are cross-sectional stiffness coefficients given by

$$\begin{aligned} &\kappa_{I33} = 2\pi \sum_{m=1}^{M} \int_{r_\mathrm{i}}^{r_0} \sigma_{I3zz} r \,\mathrm{d}r, \qquad \kappa_{I66} = 2\pi \sum_{m=1}^{M} \int_{r_\mathrm{i}}^{r_0} \sigma_{I6\theta z} r^2 \,\mathrm{d}r, \\ &\kappa_{I36} = 2\pi \sum_{m=1}^{M} \int_{r_\mathrm{i}}^{r_0} \sigma_{I6zz} r \,\mathrm{d}r = 2\pi \sum_{m=1}^{M} \int_{r_\mathrm{i}}^{r_0} \sigma_{I3\theta z} r^2 \,\mathrm{d}r \end{aligned} \tag{21}$$

and P_{I1} and M_{I1} are resultants of $\sigma_{I\mathrm{p}zz}$ and $\sigma_{I\mathrm{p}\theta z}$ of the particular solution, i.e.,

$$P_{I1} = 2\pi \sum_{m=1}^{M} \int_{r_\mathrm{i}}^{r_0} \sigma_{Ipzz} r \,\mathrm{d}r, \qquad M_{I1} = 2\pi \sum_{m=1}^{M} \int_{r_\mathrm{i}}^{r_0} \sigma_{I\mathrm{p}\theta z} r^2 \,\mathrm{d}r. \tag{22}$$

The summations in Eqs. (21) and (22) occur over M elements of the finite element model, In Eq. (20), κ_{I33} and κ_{I66} represent cross-sectional extensional and torsional rigidities of the cylinder, and κ_{I36} is the extensional/torsional coupling coefficient. For all homogeneous and laminated isotropic, orthotropic and monotropic cylinders, κ_{I36} is absent. Generic cross-sections with such material systems are structural symmetry planes, so that extensional/torsional coupling cannot exist. Moreover, no out-of-plane warpage due to an applied torque can occur, i.e., $\Psi_{I6} \equiv 0$. For any cylinder with an absence of material symmetry about its cross-section, κ_{I36}'s and cross-sectional warpage Ψ_{I6}'s will occur. Examples of such cylinders include homogeneous, anisotropic and laminated anisotropic cylinders including laminated angle-ply cylinders. Inverting $\kappa_\mathbf{I}$ in Eq. (20) gives coefficients a_{I3} and a_{I6} as

$$\begin{Bmatrix} a_{I3} \\ a_{I6} \end{Bmatrix} = \begin{bmatrix} \kappa_{I33} & \kappa_{I36} \\ \kappa_{I63} & \kappa_{I66} \end{bmatrix}^{-1} \begin{Bmatrix} P_0 - P_{I1} \\ M_0 - M_{I1} \end{Bmatrix}. \tag{23}$$

6. Problem II – linearly varying stress state

For Problem II, displacement vector $\mathbf{U}_1$ provides for a strain field that is at most linear in z. Hence, the stress field follows accordingly, and this state can accommodate linearly varying pressures and uniformly applied longitudinal and circumferential shear tractions. The governing equation on $\mathbf{U}_1$ is

$$\mathbf{K_1U}_1 + \mathbf{K_3U}_{1,z} - \mathbf{K_6U}_{1,zz} = z\mathbf{F}_1 + \mathbf{F}_0, \tag{24}$$

where $\mathbf{F}_1$ contains the pressure gradients p'_{ri} and p'_{r0} on the inner and outer surfaces, i.e., $p_{ri}(z) = zp'_{ri}$ and $p_{r0}(z) = zp'_{r0}$, and $\mathbf{F}_0$ contains the uniform longitudinal and circumferential shear tractions on the inner and outer surfaces, p_{zi}, p_{z0} and $p_{\theta i}$, $p_{\theta 0}$; see Fig. 1b. Line integrals of these tractions over the inner and outer circumferences of radii r_0 and r_i give force and torque resultants per unit length as

$$P_{z1} = 2\pi(r_0 p_{z0} - r_i p_{zi}), \qquad M_{z1} = 2\pi(r_0^2 p_{\theta 0} - r_i^2 p_{\theta i}). \tag{25}$$

The sign convention for these tractions follows that for stress as shown in Fig. 1a. The response to uniformly applied longitudinal and circumferential surface shear tractions, is embodied in the warpage components of $\mathbf{U}_1$ as will be shown. Let the tip end $z = 0$ be traction-free, so the initial values of P_z and M_z are zero. Also, assume the absence of uniform pressures as they were treated in Problem I.

The form of $\mathbf{U}_1$ is

$$\begin{aligned} u_1(r,z) &= a_{II3}(z\Psi_{I3u}(r) + \Psi_{II3u}(r)) + a_{II6}(z\Psi_{I6u}(r) + \Psi_{II5u}(r)) + b_{II3}\Psi_{I3u}(r) + b_{II6}\Psi_{I6u}(r) + zu_{II\mathrm{p}1}(r) \\ &\quad + u_{II\mathrm{p}2}(r) \\ v_1(r,z) &= \tfrac{1}{2}a_{II6}rz^2 + a_{II3}(z\Psi_{I3v}(r) + \Psi_{II3v}(r)) + a_{II6}(z\Psi_{I6v}(r) + \Psi_{II6v}(r)) + b_{II6}rz + b_{II3}\Psi_{I3v}(r) \\ &\quad + b_{II6}\Psi_{I6v}(r) + zv_{II\mathrm{p}1}(r) + v_{II\mathrm{p}2}(r) + \omega_3 r \\ w_1(r,z) &= \tfrac{1}{2}a_{II3}z^2 + a_{II3}(z\Psi_{I3w}(r) + \Psi_{II3w}(r)) + a_{II6}(z\Psi_{I6w}(r) + \Psi_{II6w}(r)) + b_{II3}z + b_{II3}\Psi_{I3w}(r) \\ &\quad + b_{II6}\Psi_{I6w}(r) + zw_{II\mathrm{p}1}(r) + w_{II\mathrm{p}2}(r) + w_0 \end{aligned} \tag{26a}$$

or in matrix notation as

$$\begin{aligned} \mathbf{U}_1 &= a_{II3}\left(\frac{z^2}{2}\mathbf{R_3} + z\boldsymbol{\Psi}_{I3} + \boldsymbol{\Psi}_{II3}\right) + a_{II6}\left(\frac{z^2}{2}\mathbf{R_4} + z\boldsymbol{\Psi}_{I6} + \boldsymbol{\Psi}_{II6}\right) + b_{II3}(z\mathbf{R_3} + \boldsymbol{\Psi}_{I3}) \\ &\quad + b_{II6}(z\mathbf{R_4} + \boldsymbol{\Psi}_{I6}) + z\mathbf{U}_{II\mathrm{p}1} + \mathbf{U}_{II\mathrm{p}2} + \omega_3\mathbf{R_4} + w_0\mathbf{R_3} \end{aligned} \tag{26b}$$

with

$$\mathbf{U}_{II\mathrm{p}1} = \begin{Bmatrix} \boldsymbol{U}_{II\mathrm{p}1} \\ \boldsymbol{V}_{II\mathrm{p}1} \\ \boldsymbol{W}_{II\mathrm{p}1} \end{Bmatrix}, \qquad \mathbf{U}_{II\mathrm{p}2} = \begin{Bmatrix} \boldsymbol{U}_{II\mathrm{p}2} \\ \boldsymbol{V}_{II\mathrm{p}2} \\ \boldsymbol{W}_{II\mathrm{p}2} \end{Bmatrix}, \qquad \Psi_{IIi} = \begin{Bmatrix} \boldsymbol{\psi}_{IIui} \\ \boldsymbol{\psi}_{IIvi} \\ \boldsymbol{\psi}_{IIwi} \end{Bmatrix}, \tag{27}$$

where $\boldsymbol{\Psi}_{Ii}$'s are Problem I warpages, $\mathbf{U}_{II\mathrm{p}1}$ and $\mathbf{U}_{II\mathrm{p}2}$ are new particular solutions for the pressure gradients, and $\boldsymbol{\Psi}_{IIi}$'s are new warpage functions. Displacement field (26b) is obtained by integrating the displacement field (14b) of Problem I once with respect to z and introducing new kinematic coefficients (a_{II3}, a_{II6}) and (b_{II3}, b_{II6}). As noted earlier, this method for generating the displacement field is due to Ieşan (1986,1987).

To determine the new kinematic data, substitute displacement field (26b) into equilibrium equation (24).

$$\begin{aligned} &z^2 a_{II3}\{\mathbf{K_1R_3}\} + z^2 a_{II6}\{\mathbf{K_1R_4}\} + z a_{II3}\{\mathbf{K_1}\boldsymbol{\Psi}_{I3} + \mathbf{K_3R_3}\} + z a_{II6}\{\mathbf{K_1}\boldsymbol{\Psi}_{I6} + \mathbf{K_3R_4}\} + z b_{II3}\{\mathbf{K_1R_3}\} \\ &\quad + z b_{II6}\{\mathbf{K_1R_4}\} + z\{\mathbf{K_1U}_{II\mathrm{p}1} - \mathbf{F}_1\} + a_{II3}\{\mathbf{K_1}\boldsymbol{\Psi}_{II3} + \mathbf{K_3}\boldsymbol{\Psi}_{I3} - \mathbf{K_6R_3}\} + a_{II6}\{\mathbf{K_1}\boldsymbol{\Psi}_{II6} + \mathbf{K_3}\boldsymbol{\Psi}_{I6} - \mathbf{K_6R_4}\} \\ &\quad + b_{II3}\{\mathbf{K_1}\boldsymbol{\Psi}_{I3} + \mathbf{K_3R_3}\} + b_{II6}\{\mathbf{K_1}\boldsymbol{\Psi}_{I6} + \mathbf{K_3R_4}\} + \{\mathbf{K_1U}_{II\mathrm{p}2} + \mathbf{K_3U}_{II\mathrm{p}1} - \mathbf{F}_0\} = 0 \end{aligned} \tag{28}$$

Each term in Eq. (28) enclosed by braces must vanish. Many of the terms reiterate rigid body identities (13) and Eq. (17) for the warpages of Problem I. The equations providing new data are

$$\begin{aligned} \mathbf{K_1}\boldsymbol{\Psi}_{II3} &= -\mathbf{K_3}\boldsymbol{\Psi}_{I3} + \mathbf{K_6}\mathbf{R_3}, \qquad & \mathbf{K_1}\mathbf{U}_{II\mathrm{p}1} &= \mathbf{F}_1, \\ \mathbf{K_1}\boldsymbol{\Psi}_{II6} &= -\mathbf{K_3}\boldsymbol{\Psi}_{I6} + \mathbf{K_6}\mathbf{R_4}, \qquad & \mathbf{K_1}\mathbf{U}_{II\mathrm{p}2} &= \mathbf{F}_0 - \mathbf{K_3}\mathbf{U}_{II\mathrm{p}1}. \end{aligned} \tag{29}$$

Solving Eq. (29) gives the warpages $\boldsymbol{\Psi}_{II3}$ and $\boldsymbol{\Psi}_{II6}$ and particular solutions $\mathbf{U}_{II\mathrm{p}2}$ and $\mathbf{U}_{II\mathrm{p}1}$.

It was noted that an axial and a hoop degree of freedom must be restrained in $\mathbf{K_1}$ to suppress its singular nature. In Problem II, the restrained degree of freedom identifies the surface where the shear tractions are applied. The solution of Eq. (29) for warpages $\boldsymbol{\Psi}_{II3}$ and $\boldsymbol{\Psi}_{II6}$ gives a stress field that acts as *applied loads*, while the restrained degree of freedom plays the role of a *support* or *reaction*. This reversal of roles is permissible since a rigid body displacement can be appended to satisfy any prescribed kinematic conditions at the fixed end of the cylinder. Only one pair of traction components on a lateral surface can be accommodated with each set of warpages. For two loaded surfaces, superposition must be used.

The strain and stress distributions from Eqs. (26a), (26b), (4) and (1) are

$$\begin{aligned} \boldsymbol{\epsilon} &= a_{II3}(z\boldsymbol{\epsilon}_{I3} + \boldsymbol{\epsilon}_{II3}) + a_{II6}(z\boldsymbol{\epsilon}_{I6} + \boldsymbol{\epsilon}_{II6}) + z\boldsymbol{\epsilon}_{II\mathrm{p}1} + \boldsymbol{\epsilon}_{II\mathrm{p}2}, \\ \boldsymbol{\sigma} &= a_{II3}(z\boldsymbol{\sigma}_{I3} + \boldsymbol{\sigma}_{II3}) + a_{II6}(z\boldsymbol{\sigma}_{I6} + \boldsymbol{\sigma}_{II6}) + z\boldsymbol{\sigma}_{II\mathrm{p}1} + \boldsymbol{\sigma}_{II\mathrm{p}2}, \end{aligned} \tag{30}$$

where $(\boldsymbol{\epsilon}_{I3}, \boldsymbol{\epsilon}_{I6}, \boldsymbol{\sigma}_{I3}, \boldsymbol{\sigma}_{I6})$ were given by Eq. (19) and

$$\begin{aligned} \boldsymbol{\epsilon}_{II3} &= \mathbf{b}_r\boldsymbol{\Psi}_{II3} + \mathbf{b}_z\boldsymbol{\Psi}_{I3}, \qquad & \boldsymbol{\sigma}_{II3} &= \mathbf{C}\boldsymbol{\epsilon}_{II3}, \\ \boldsymbol{\epsilon}_{II6} &= \mathbf{b}_r\boldsymbol{\psi}_{II6} + \mathbf{b}_z\boldsymbol{\psi}_{I6}, \qquad & \boldsymbol{\sigma}_{II6} &= \mathbf{C}\boldsymbol{\epsilon}_{II6}, \\ \boldsymbol{\epsilon}_{II\mathrm{p}1} &= \mathbf{b}_r\mathbf{u}_{II\mathrm{p}1}, \qquad & \boldsymbol{\sigma}_{II\mathrm{p}1} &= \mathbf{C}\boldsymbol{\epsilon}_{II\mathrm{p}1}, \\ \boldsymbol{\epsilon}_{II\mathrm{p}2} &= \mathbf{b}_r\mathbf{u}_{II\mathrm{p}2} + \mathbf{b}_z\mathbf{u}_{II\mathrm{p}1}, \qquad & \boldsymbol{\sigma}_{II\mathrm{p}2} &= \mathbf{C}\boldsymbol{\epsilon}_{II\mathrm{p}2.} \end{aligned} \tag{31}$$

Integrating $\sigma_{zz}(z)$ and $\sigma_{z\theta}(z)$ over the cross-section according to Eq. (9) gives the axial force $P_z(z)$ and torque $M_z(z)$ at any arbitrary station along the z-axis as

$$\begin{aligned} \begin{Bmatrix} P_z(z) \\ M_z(z) \end{Bmatrix} = z\left(\begin{bmatrix} \kappa_{I33} & \kappa_{I63} \\ \kappa_{I63} & \kappa_{I66} \end{bmatrix} \begin{Bmatrix} a_{II3} \\ a_{II6} \end{Bmatrix} + \begin{Bmatrix} P_{II1} \\ M_{II1} \end{Bmatrix} \right) \begin{bmatrix} \kappa_{II33} & \kappa_{II63} \\ \kappa_{II63} & \kappa_{II66} \end{bmatrix} \begin{Bmatrix} a_{II3} \\ a_{II6} \end{Bmatrix} + \begin{bmatrix} \kappa_{I33} & \kappa_{I63} \\ \kappa_{I63} & \kappa_{I66} \end{bmatrix} \begin{Bmatrix} b_{II3} \\ b_{II6} \end{Bmatrix} \\ + \begin{Bmatrix} P_{II2} \\ M_{II2} \end{Bmatrix}, \end{aligned} \tag{32}$$

where coefficients κ_{Iij}'s are those of Problem I. Coefficients κ_{IIij}'s and resultants P_{II2}, M_{II2}, P_{II1}, M_{II1} arise from integrating the σ_{zz} and $\sigma_{\theta z}$ components of $\boldsymbol{\sigma}_{II3}$, $\boldsymbol{\sigma}_{II6}$, $\boldsymbol{\sigma}_{II\mathrm{p}2}$ and $\boldsymbol{\sigma}_{II\mathrm{p}1}$ according to formulas analogous to Eqs. (21) and (22).

Global equilibrium mandates vanishing of the sums of the derivatives of $P_z(z)$ and $M_z(z)$ and the resultants P_{z1} and M_{z1} of the applied surface tractions,

$$\frac{\partial P_z}{\partial z} + P_{z1} = 0 \quad \text{and} \quad \frac{\partial M_z}{\partial z} + M_{z1} = 0 \tag{33}$$

with P_{z1} and M_{z1} given by Eq. (25). Differentiating Eq. (32) with respect to z and invoking Eq. (33) yield the following equation for a_{II3} and a_{II6}.

$$\begin{Bmatrix} a_{II3} \\ a_{II6} \end{Bmatrix} = -\begin{bmatrix} \kappa_{I33} & \kappa_{I36} \\ \kappa_{I63} & \kappa_{I66} \end{bmatrix}^{-1} \begin{Bmatrix} P_{z1} + P_{II1} \\ M_{z1} + M_{II1} \end{Bmatrix}. \tag{34}$$

Then, b_{II3} and b_{II6} can be determined from Eq. (32) by invoking initial conditions $P_z = M_z = 0$ at $z = 0$.

$$\begin{Bmatrix} b_{II3} \\ b_{II6} \end{Bmatrix} = -\begin{bmatrix} \kappa_{I33} & \kappa_{I63} \\ \kappa_{I63} & \kappa_{I66} \end{bmatrix}^{-1} \left(\begin{bmatrix} \kappa_{II33} & \kappa_{II63} \\ \kappa_{II63} & \kappa_{II66} \end{bmatrix} \begin{Bmatrix} a_{II3} \\ a_{II6} \end{Bmatrix} + \begin{Bmatrix} P_{II2} \\ M_{II2} \end{Bmatrix} \right). \tag{35}$$

7. Examples

Consider a two-layer ±30° angle-ply laminate of equal thickness plies of a fiber composite material whose mechanical properties are

$$\frac{E_L}{E_T}=20,\qquad \frac{G_{LT}}{E_T}=0.4,\qquad \frac{G_{TT}}{E_T}=0.3,\qquad \nu_{TT}=0.3,\qquad \nu_{LT}=0.2. \tag{36}$$

These properties in terms of coefficients C_{ij}'s at ±30° orientations with the coordinate axes are

$$\mathbf{C_{ij}}=E_T\begin{bmatrix} 2.28538 & 0.32217 & 3.85796 & \cdot & \pm 2.05471 & \cdot \\ 0.32217 & 1.10301 & 0.29896 & \cdot & \mp 0.02010 & \cdot \\ 3.85796 & 0.29896 & 11.7913 & \cdot & \pm 6.17768 & \cdot \\ \cdot & \cdot & \cdot & 0.37500 & \cdot & \pm 0.04330 \\ \pm 2.05471 & \mp 0.02010 & \pm 6.17768 & \cdot & 3.97060 & \cdot \\ \cdot & \cdot & \cdot & \pm 0.04330 & \cdot & 0.32500 \end{bmatrix}_{\pm 30^\circ}. \tag{37}$$

To illustrate the differences in the behaviors between a thick-walled cylinder and a shell, two radius/thickness ratios are considered, $R/H=1$ and 10, where H is the total laminate thickness and R is the mean radius of the cylinder. The cross-sectional stiffness matrices, $\boldsymbol{\kappa}_\mathbf{I}$'s, for these two cylinders are

$$\kappa_\mathbf{I}=E_T H^2\begin{bmatrix} 26.187 & 27.957H \\ \text{sym} & 114.28H^2 \end{bmatrix}_{R/H=1},\qquad \kappa_\mathbf{I}=E_T H^2\begin{bmatrix} 212.053 & 292.818H \\ \text{sym} & 98058.4H^2 \end{bmatrix}_{R/H=10}, \tag{38}$$

where these values are valid only for their given R/H ratios.

8. Problems I loads

For loading conditions of axial force P_0, torque M_0 and external pressure p_0, the coefficients, a_{I3} and a_{I6}, for unit values of these loads are listed in Table 1. Normalized displacement and stress distributions are shown in Figs. 2–6, where the normalization factors, $\overline{u}$ and $\overline{\sigma}$, for three loading conditions are listed in Table 2. The only non-zero warpage component for axial force and torque is the radial component as shown in Fig. 1. The primal field components, $w_0=a_{I3}z$ and $v_0=a_{I3}rz$, are not shown. The normalized stress components $\sigma_{ij}/\overline{\sigma}$ for axial force and torque are shown in Figs. 3 and 4. Note interlaminar kinks (or jumps) in σ_{zz} under axial force P_0 and in $\sigma_{\theta z}$ under torque M_0, even though C_{33} and C_{44} are the same for both layers in this angle-ply layup. This behavior is attributable to anisotropy, as C_{35} and C_{46} are different in the two layers. The jumps are small for the shell, $R/H=10$, vis-a-vis those in the thick-walled cylinder,

Table 1
Summary of a_{I3} and a_{I6} coefficients for $P_0=1$, $M_0=1$, $p_0=1$

	$R/H=1$		$R/H=10$	
	a_{I3}	a_{I6}	a_{I3}	a_{I6}
Axial force	0.05169	−0.01264	47.353×10^{-4}	-0.1414×10^{-4}
Torque	−0.01264	0.01184	-0.1414×10^{-4}	0.1024×10^{-4}
Uniform pressure	0.8126	−0.1393	6.2889	−0.01624

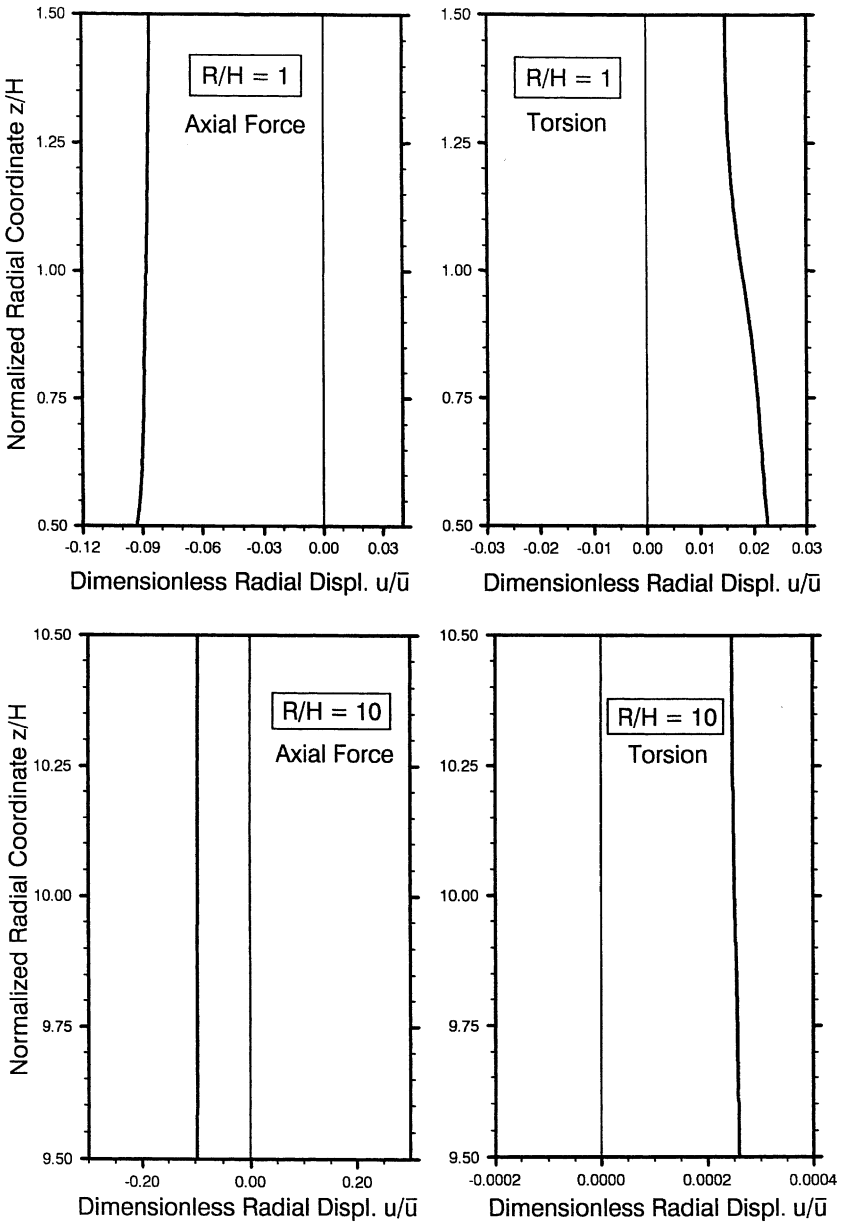

Fig. 2. Normalized radial displacement for axial force P_0 and Torque M_0.

$R/H = 1$. As $R/H \rightarrow$ large, i.e., retreating into the thin shell regime, these jumps, while always present because of coupling from anisotropy, will be even less noticeable and give an appearance of a quasi linear stress distribution. Plots of the radial displacement and stresses for unit external pressure are shown in Figs. 5 and 6. Again, the primal displacement field, $w_0 = a_{13}z$ and $v_0 = a_{13}rz$, that is coupled with pressurization is not shown. Due extension-shear coupling, shear stress $\sigma_{\theta z}$ accompanies the normal stress components for external pressurization, and there are jumps of $\sigma_{\theta\theta}$, σ_{zz} and $\sigma_{\theta z}$ at the interlaminar surface.

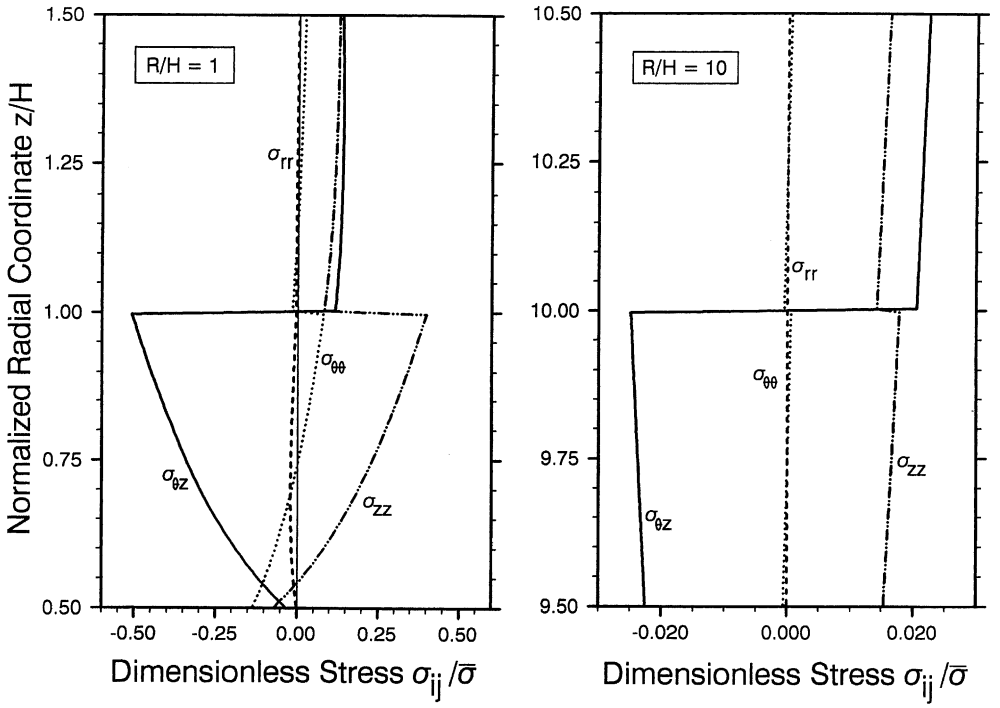

Fig. 3. Normalized stress for axial force P_0.

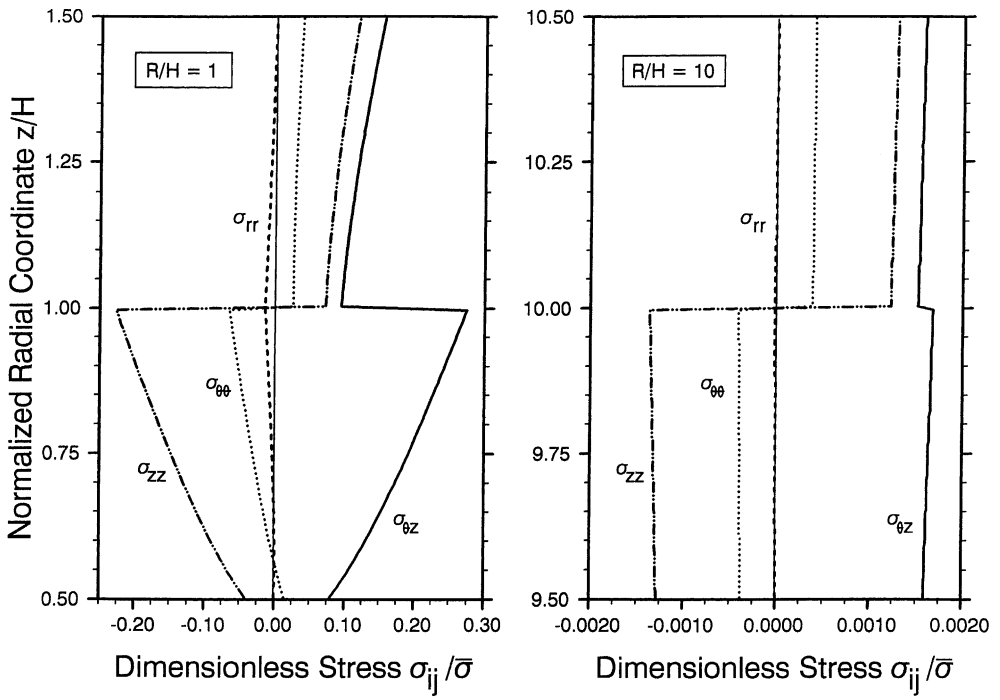

Fig. 4. Normalized stress for torque M_0.

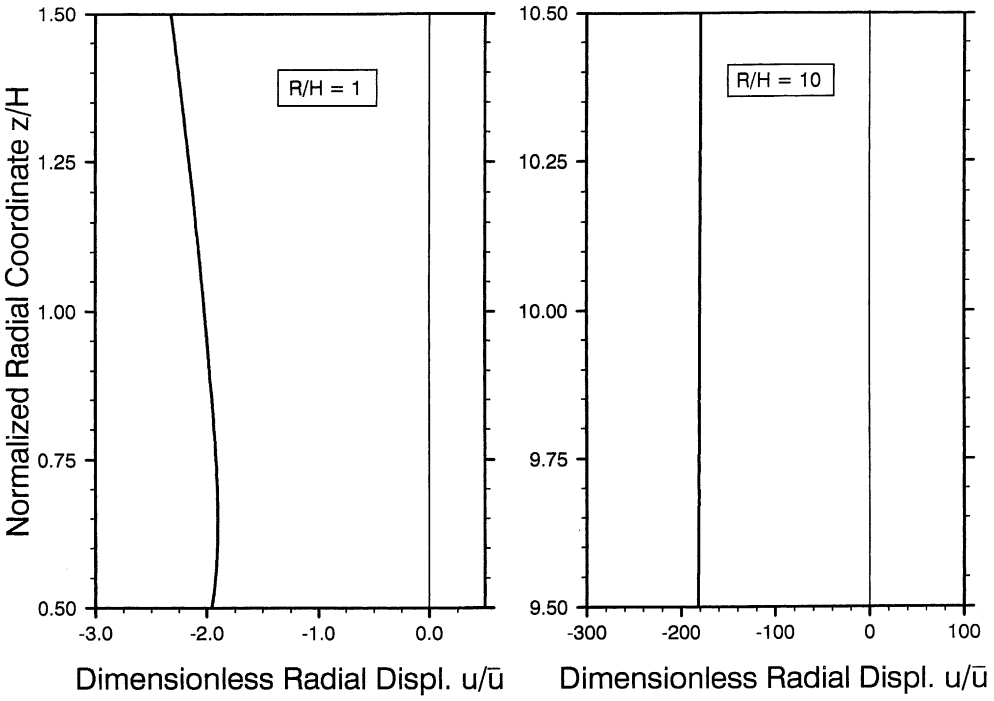

Fig. 5. Normalized radial displacement for uniform external pressure p_0.

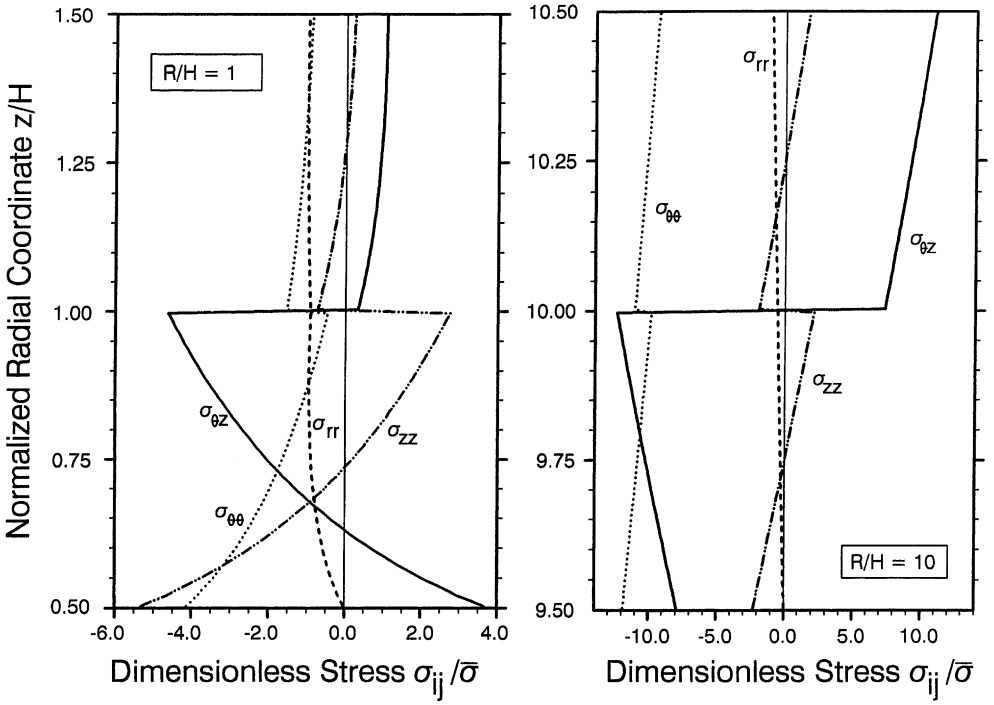

Fig. 6. Normalized stress for uniform external pressure p_0.

Table 2
Normalization factor for various loads

Axial force	Torque	Uniform ext. pressure
$\overline{u} = P_0/E_T H$	$\overline{u} = M_0/E_T H^2$	$\overline{u} = p_0 H/E_T$
$\overline{\sigma} = P_0/H^2$	$\overline{\sigma} = M_0/H^3$	$\overline{\sigma} = p_0$
Linear pressure	Uniform cir. shear	Uniform long. shear
$\overline{u}_1 = p_0 H^2/E_T$	$\overline{u}_1 = p_{\theta 0} H/E_T$	$\overline{u}_1 = p_{z0} H/E_T$
$\overline{\sigma}_1 = p_0 H$	$\overline{\sigma}_1 = p_{\theta 0}$	$\overline{\sigma}_1 = p_{z0}$
$\overline{u}_2 = p_0 H/E_T$	$\overline{u}_2 = p_{\theta 0}/E_T$	$\overline{u}_2 = p_{z0}/E_T$
$\overline{\sigma}_2 = p_0$	$\overline{\sigma}_2 = p_{\theta 0}/H$	$\overline{\sigma}_2 = p_{z0}/H$

Table 3
Summary of a_{II3} and a_{II6} coefficients for $p'_{r0} = 1$, $p_{\theta 0} = 1$, $p_{z0} = 1$

	$R/H = 1$		$R/H = 10$	
	a_{II3}	a_{II6}	a_{II3}	a_{II6}
Linear pressure	0.8126	−0.1393	6.2889	−0.01624
Uniform cir. shear	0.1788	−0.1674	97.95×10^{-4}	-70.94×10^{-4}
Uniform long. shear	−0.4871	0.1192	−0.3124	9.3289×10^{-4}

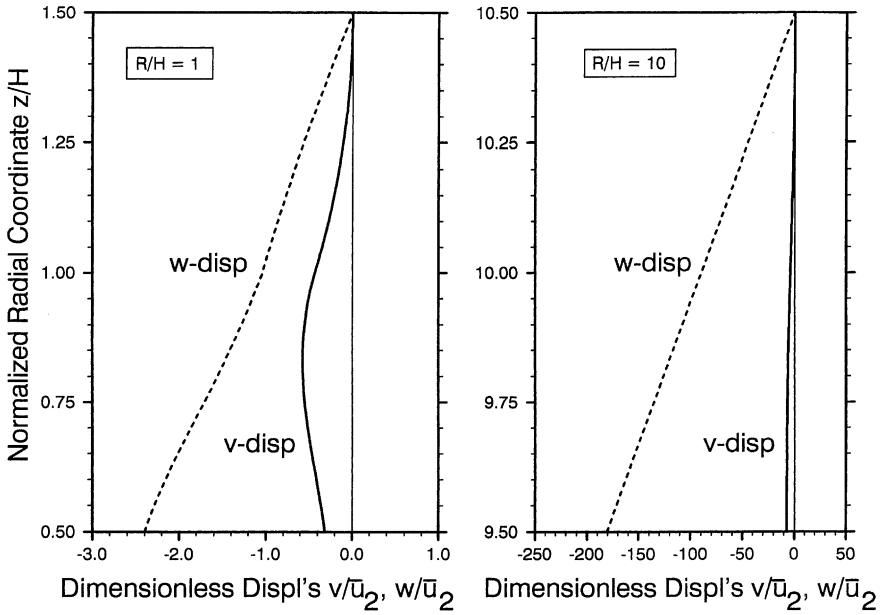

Fig. 7. Normalized radial displacement for linearly varying external pressure p'_{r0}.

9. Problem II loads

For loading conditions of linearly varying external pressure of rate p'_{r0}, uniform external circumferential shear $p_{\theta 0}$, and uniform external longitudinal shear p_{z0}, all $\boldsymbol{\kappa}_{II}$'s are zero; therefore, $b_{II3} = b_{II6} = 0$. The values of a_{II3} and a_{II6} for unit values of these loads are listed in Table 3.

Normalized displacement and stress plots are shown in Figs. 7–12 for the three loading conditions. The two sets of normalization factors, one for displacement and stress gradients, $\overline{u}_1$ and $\overline{\sigma}_1$, and the other for displacements and stresses uniform in the axial direction, $\overline{u}_2$ and $\overline{\sigma}_2$, are listed Table 2. In Figs. 7, 9, and 11 are plots of the normalized displacements uniform in the axial direction for the three loading conditions, i.e.,

$$U_1 = a_{II3}\boldsymbol{\Psi}_{II3} + a_{II6}\boldsymbol{\Psi}_{II6} + \mathbf{U}_{II\mathrm{p}2}. \tag{39}$$

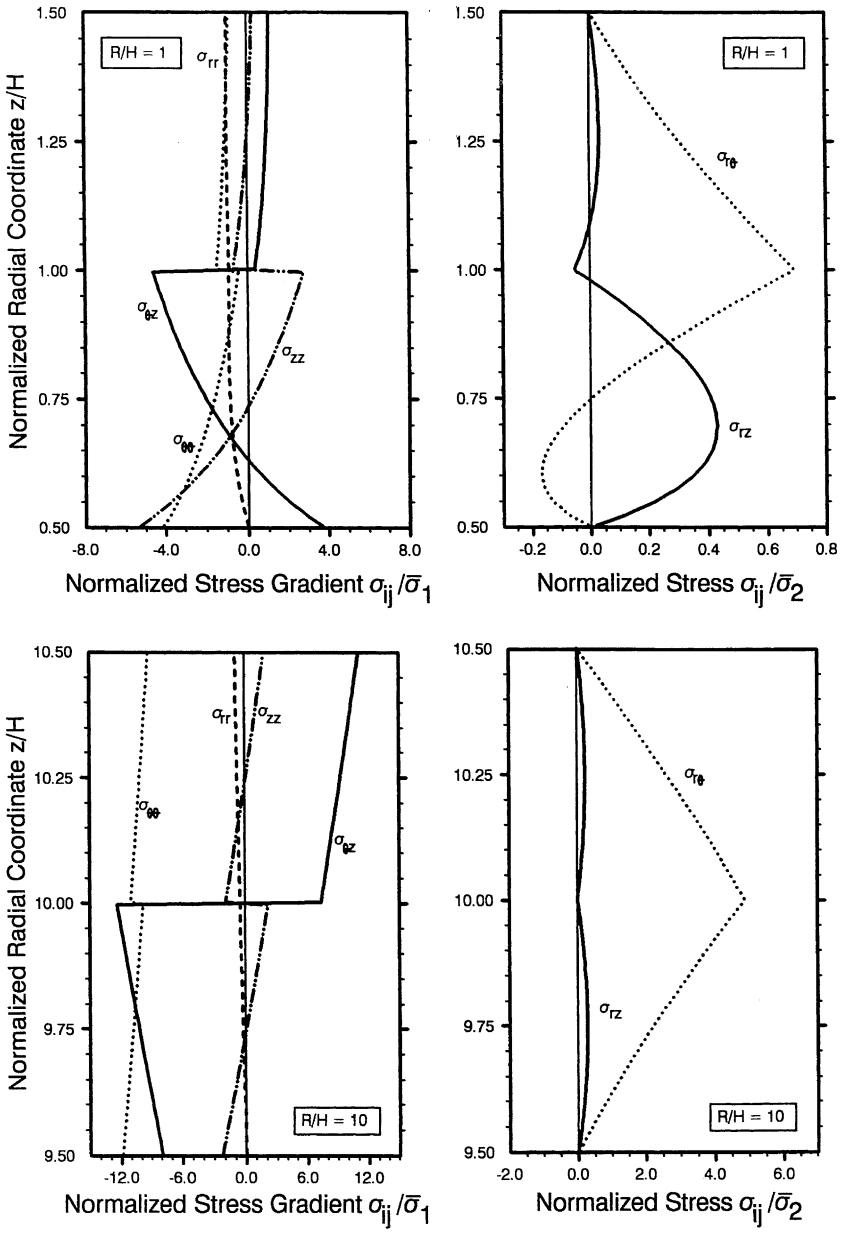

Fig. 8. Normalized stress for linearly varying external pressure p'_{r0}.

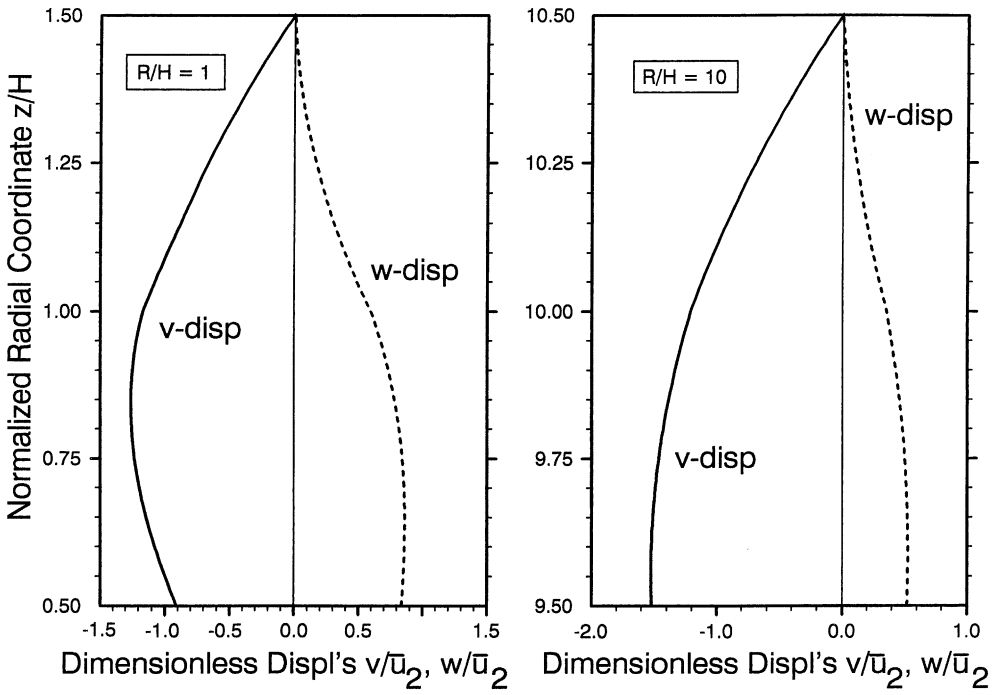

Fig. 9. Normalized displacements for uniform external circumferential shear p_{00}.

In all cases, the radial component is identically zero. Note that the circumferential and longitudinal displacements on the outer surface are zero in all cases, as explained by their reversal of roles. The total displacement on the outer surface will not be zero because a rigid body displacement will be appended to satisfy end conditions at $z = L$. The normalized stress gradients are presented in Figs. 8, 10, 12. Since unit loads were used and the stress gradients are linear combinations of σ_{I3} and σ_{I6}, i.e.,

$$\boldsymbol{\sigma}_{\mathbf{I}} = z\left[a_{II3}\boldsymbol{\sigma}_{I3} + a_{II6}\boldsymbol{\sigma}_{I6} + \boldsymbol{\sigma}_{II\mathrm{p1}}\right] \tag{40}$$

all graphs show the same distributions, except for the sign, as those for axial force, torque and uniform external pressure of Problem I. The sign difference of the two sets of plots is due to the fact that the uniform outer surface tractions produce a compressive axial force and negative torque, whereas the plots for Problem I are for a tensile axial force and positive torque. Plots of the normalized uniform stress components, i.e.,

$$\boldsymbol{\sigma}_{\mathbf{II}} = a_{II3}\boldsymbol{\sigma}_{II3} + a_{II6}\boldsymbol{\sigma}_{II6} + \boldsymbol{\sigma}_{II\mathrm{p2}} \tag{41}$$

are shown in Figs. 8, 10, and 12. For a shell, $R/H = 10$, the circumferential and longitudinal shear stresses appear to vary linearly over the laminate thickness profile, while that for the thick-walled cylinder, $R/H = 1$, they are curvilinear.

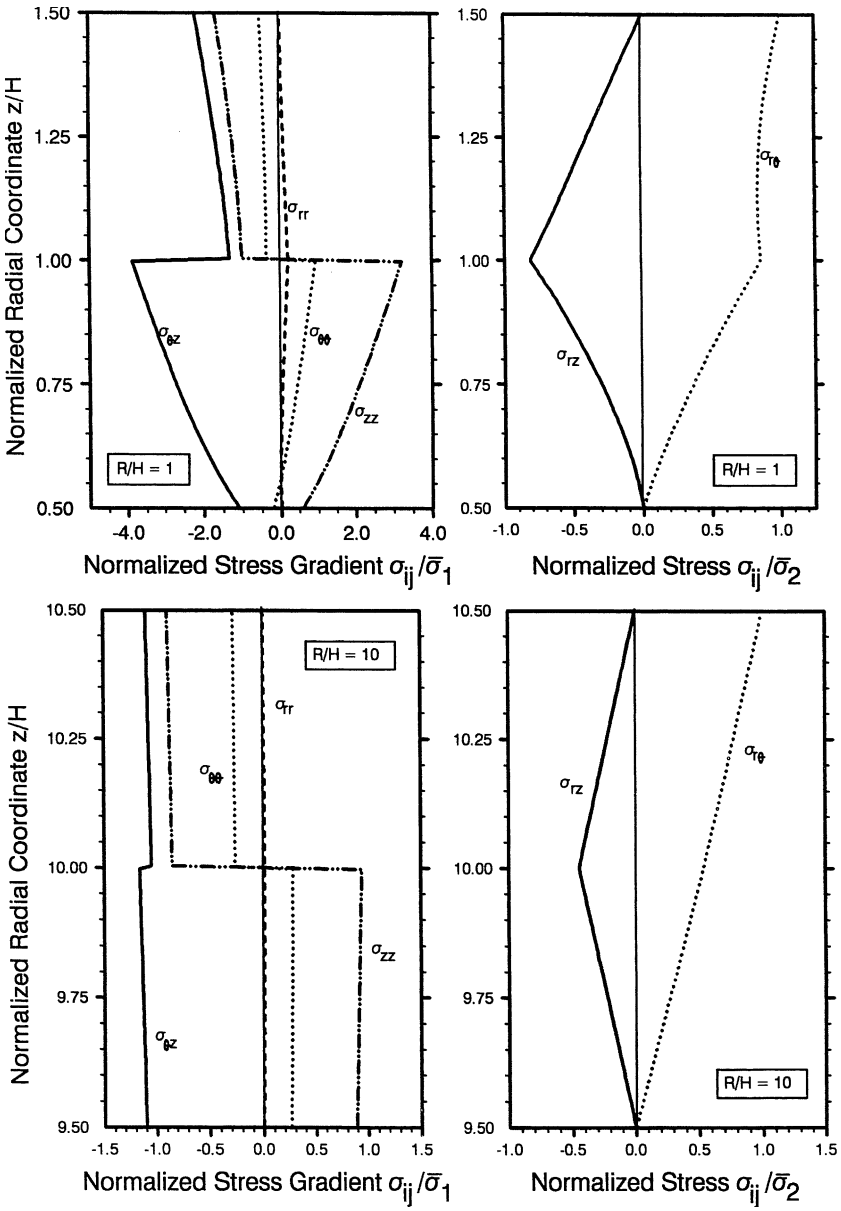

Fig. 10. Normalized stress for uniform external circumferential shear p_{00}.

10. Concluding remarks

A solution procedure for axisymmetric stresses and deformations in a laminated circular cylinder of materials with the most general form of cylindrical anisotropy was presented. The governing equation is based on a semi-analytical finite element formulation with the axial dependence z left in analytic form. The solution methodology calls for the decomposition of the loading into power series of z with each load term

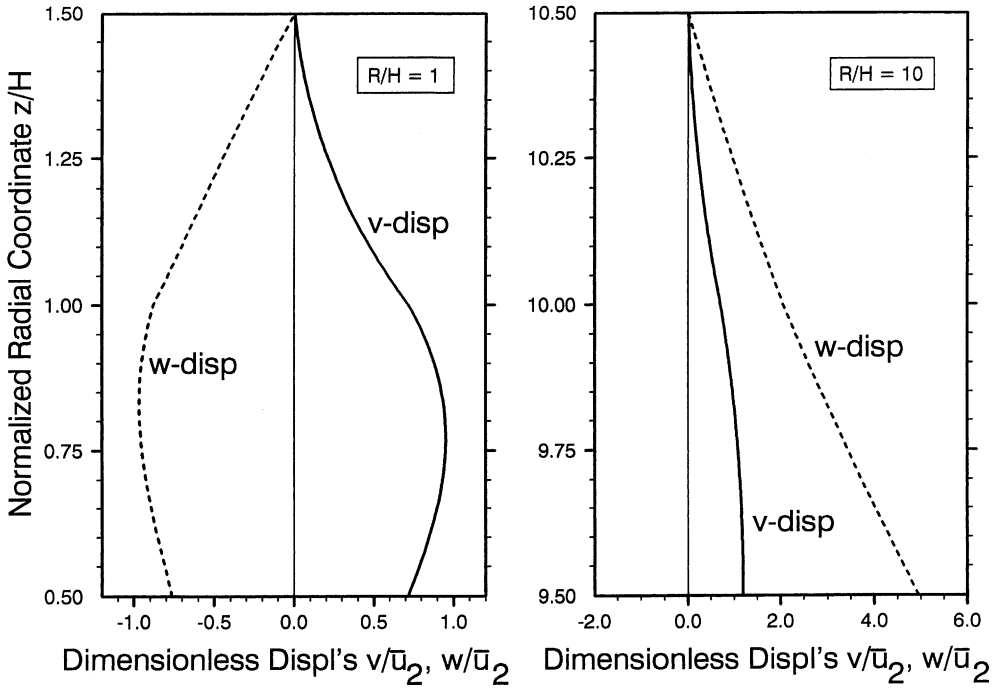

Fig. 11. Normalized displacements for uniform external longitudinal shear p_{z0}.

comprising a problem. The total response is sought in ascending order of this load series with the first two terms relating to uniform pressurization and linear pressurization with uniform circumferential and longitudinal surface shears. From solution details for these terms, the methodology for subsequent terms should be straight-forward. The behaviors of a thin and thick two-layer $\pm 30^\circ$ angle-ply cylinder were presented to contrast some unusual phenomena in them.

The present solutions are based on a relaxed formulation where integral end conditions are used rather than a point-wise specification. A solution based on a point-wise specification of the end conditions will only show differences in the vicinity of the ends according to Saint-Venant's principle. The difference is merely a self-equilibrated state which attenuates with distance into the interior of the cylinder. This self-equilibrated state can be represented by an eigenvector expansion with eigendata extracted from the following quadratic eigenproblem:

$$\mathbf{K_1 U} - \gamma \mathbf{K_3 U} - \gamma^2 \mathbf{K_6 U} = 0, \tag{42}$$

where γ is the inverse decay length parameter. Eigenproblem (42) is obtained by substituting the displacement field $\mathbf{U}(z) = \mathbf{U}e^{-\gamma z}$ into the homogeneous form of Eq. (6). The underpinnings for the derivation of Eq. (42) are the strain energy decay inequality theorems of Toupin (1965) and Knowles (1966). It is mentioned that the dynamic counterpart of Eq. (42) relates to steady-state edge vibrations, which have been discussed by Huang and Dong (1984) and Zhuang et al. (1999). Elastostatic end solution data from their formulations may be extracted by setting the steady-state frequency $\omega = 0$. No examples of self-equilibrated end effects were given herein; but Kazic and Dong (1990) and Lin et al. (2001) have illustrated analyses of end effects for restrained torsion and other end loads in beams with arbitrarily-shaped cross-sections.

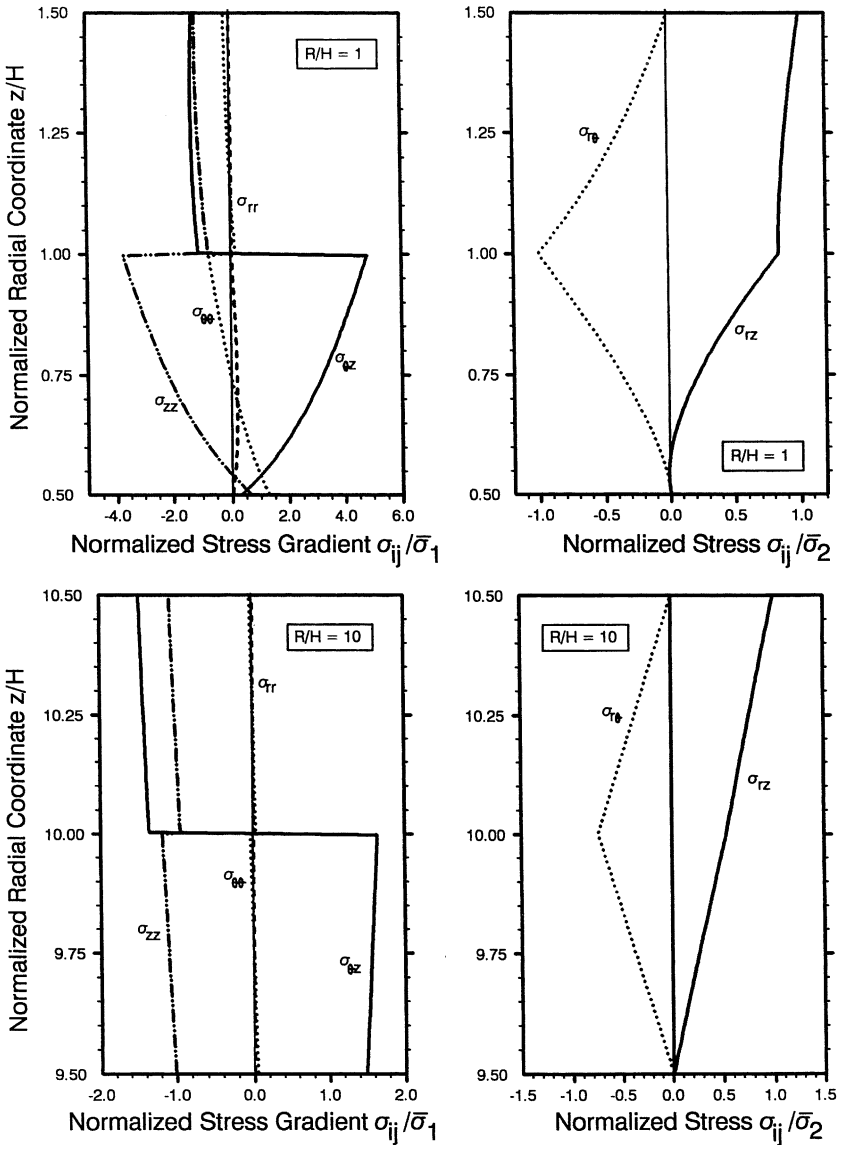

Fig. 12. Normalized stress for uniform external longitudinal shear p_{z0}.

References

Almansi, E., 1901a. Sopra la deformazione dei cilinri solecitati lateralmente. Atti Real Accad. naz. Lincei Rend, Cl. sci fis., mat e natur. Ser. 5 10 (I), 333–338.

Almansi, E., 1901b. Sopra la deformazione dei cilinri solecitati lateralmente. Atti Real Accad. naz. Lincei Rend, Cl. sci fis., mat e natur. Ser. 5 10 (II), 400–408.

Chandrashekhara, K., Gopalakrishnan, P., 1982. Elasticity solution for a multilayered transversely isotropic circular cylindrical shell. J. Appl. Mech. ASME 49 (1), 108–114.

Chou, F.H., Achenbach, J.D., 1972. Three dimensional vibration of orthotropic cylinders. J. Engng. Mech. Div. ASCE 98 (EM4), 813–822.

Grigorenko, Ya.M., Vasilenko, A.T., Pankratova, N.D., 1974. Computation of the stressed state of thick-walled inhomogeneous, anisotropic shells. Prikladnaya Mekhanika 10, 86–93.
Huang, K.H., Dong, S.B., 1984. Propagating waves and standing vibrations in a composite cylinder. J. Sound Vib. 96 (3), 363–379.
Hyer, M.W., 1988. Hydrostatic response of thick laminated composite cylinders. J. Reinfor. Plastics Compos. 7, 321–340.
Hyer, M.W., Cooper, D.E., Cohen, D., 1986. Stresses and deformations in cross-ply composite tubes subjected to uniform temperature change. J. Thermal Stresses 9, 97–117.
Hyer, M.W., Rousseau, C.Q., 1987. Thermally induced stresses and deformations in angle-ply composite tubes. J. Comp. Mat. 21 (5), 454–480.
Ieşan, D., 1986. On Saint-Venant's problem. Arch. Ration. Mech. Anal. 91, 363–373.
Ieşan, D., 1987. Saint-Venant's problem. Lectures Notes in Mathematics, Springer, Heidelberg.
Kazic, M., Dong, S.B., 1990. Analysis of restrained torsion. J. Engng. Mech. Div. 116 (4), 870–891.
Knowles, J.K., 1966. On Saint-Venant's principle in the two-dimensional linear theory of elasticity. Arch. Ration. Mech. Anal. 21, 1–22.
Kollar, L.P., Springer, G.S., 1992. Stress analysis of anisotropic laminated cylinders and cylindrical segments. Int. J. Solids Struct. 29 (12), 1499–1517.
Kollar, L.P., Patterson, J.M., Springer, G.S., 1992. Composite cylinders subjected to hygrothermal and mechanical loads. Int. J. Solids Struct. 29 (12), 1519–1534.
Kollar, L.P., Patterson, J.M., 1993. Composite cylindrical segments subjected to hygrothermal and mechanical loads. Int. J. Solids Struct. 30 (18), 2525–2545.
Kollar, L.P., 1994. Three-dimensional analysis of composite cylinders under axially varying hygrothermal and mechanical loads. Comput. Struct. 50 (4), 525–540.
Lee, S.Y., Springer, G.S., 1990. Filament winding cylinders: I. Process model. J. Comp. Mat. 24, 1270–1298.
Lekhnitskii, S.G., 1981. Theory of Elasticity of an Anisotropic Body. Mir Publishers, Moscow (translated from the revised 1977 Russian edition).
Lin, H.C., Dong, S.B. Dong, Kosmatka, J.B., 2001. On Saint-Venant's problem for an inhomogeneous, anisotropic cylinder. J. Appl. Mech., in press.
Michell, J.H., 1901. The theory of uniformly loaded beams. Quart. J. Math. 32, 28–42.
Noor, A.K., Rarig, P.L., 1974. Three dimensional solutions of laminated cylinders. Comput. Meth. Appl. Mech. Engng. 3, 319–334.
Noor, A.K., Peters, J.M., 1989. Stress, vibration and buckling of multilayered cylinders. J. Struct. Engng. 115 (1), 69–88.
Noor, A.K., Burton, W.S., Peters, J.M., 1991. Assessment of computational models for multilayered composite cylinders. Int. J. Solids Struct. 27 (10), 1269–1286.
Pagano, N.J., 1972. The stress field in a cylindrically anisotropic body under two-dimensional surface tractions. J. Appl. Mech. 39 (3), 791–796.
Ren, J.G., 1987. Exact solutions for laminated cylindrical shells in cylindrical bending. Comp. Sci. Tech. 29, 169–187.
Roy, A.K., Tsai, S.W., 1988. Design of thick composite cylinders. J. Pressure Vessel Tech. 110 (3), 255–262.
de Saint-Venant, A.J.C.B., 1856a. Memoire sur la torsion des prismes. Memoires des Savants etrangers 14, 233–560.
de Saint-Venant, A.J.C.B., 1856b. Memoire sur la flexion des prismes. J. de Mathematiques de Liouville Ser. II 1, 89–189.
Shaffer, B.W., 1968. Pressurization of two-layered incompressible orthotropic tubes. J. Frank. Inst. 285, 187–203.
Sherrer, R.E., 1967. Filament-wound cylinders with axial-symmetric loads. J. Comp. Mat. 1, 344–355.
Spencer, A.J.M., Watson, P., Rogers, T.G., 1990. Stress analysis of anisotropic laminated circular cylindrical shells. In: Hui, D., Sun, C.T. (Eds.), Recent Developments in Composite Materials Structures, Aerospace Div., ASME, vol. 19, pp. 57–60.
Srinivas, S., 1974. Analysis of laminated composite circular cylindrical shells with general boundary conditions, NASA TR-R-412.
Toupin, R.A., 1965. Saint-Venant's principle. Arch. Ration. Mech. Anal. 18, 83–96.
Varadan, T.K., Bhaskar, K., 1991. Bending of laminated ortho-tropic cylindrical shells-an elastic approach. Compos. Struct. 17 (2), 141–156.
Ye, J., Soldatos, K.P., 1994. Three-dimensional stress analysis of orthotropic and cross-ply laminated hollow cylinders and cylindrical panels. Comp. Meth. Appl. Mech. Engng. 117, 331–351.
Zhuang, W., Shah, A.H., Dong, S.B., 1999. Elastodynamic Green's function for laminated anisotropic circular cylinders. J. Appl. Mech. 66 (3), 665–674.